

## Article

# Stability Influencing Factors and Control Methods of Residual Coal Pillars with Solid Waste Materials Backfilling Method

Shan Ning<sup>1</sup>, Jinfu Lou<sup>2</sup>, Laolao Wang<sup>1,3,\*</sup> , Dan Yu<sup>1</sup>  and Weibing Zhu<sup>1,\*</sup> 

<sup>1</sup> State Key Laboratory of Coal Resources and Safe Mining, China University of Mining and Technology, Xuzhou 221116, China

<sup>2</sup> CCTEG, Coal Mining Research Institute, Beijing 100013, China

<sup>3</sup> Institute of Mining Engineering and Geology, Xinjiang Institute of Engineering, Urumqi 830023, China

\* Correspondence: ts18020047a3tm1@cumt.edu.cn (L.W.); cumtzwb@cumt.edu.cn (W.Z.)

**Abstract:** Affected by coal mining activities, the remaining coal pillars are very likely to be destabilized and cause safety accidents. The backfilling of the remaining goaf can maintain the stability of the coal pillar well, but the coal pillar in the unfilled zone may still be unstable. In this paper, the effect of backfilling materials on coal pillars and the reinforcement method are discussed using numerical simulation, statistical mathematics, elastic mechanics, and mechanical test methods. The results show that: backfilling with solid waste materials and reinforcing the coal pillar could maintain the stability of the bottom goaf, where the backfill body height is the main factor in the strength of the coal pillar. The propagation of the confining stress of the backfill body on the pillar in the unfilled zone is the primary way to influence the coal pillar strength. Changing the backfill body height filling can affect the coal pillar strength. By analyzing the propagation law of confining stress in the coal pillar, the minimum backfill body height is determined to be 7 m. Combined with mechanical tests and the Mohr–Coulomb criterion, the minimum confining pressure required to maintain the coal pillar stability under the peak ground pressure is analyzed. The ratio of solid waste materials is determined based on this. Field tests have proved that the coal pillar remains stable when the goaf is not filled, and the cement/fly ash ratio is 1:4, which can ensure product safety. The research has significant value and significance for the governance of the remaining coal pillars and production safety.

**Keywords:** confining strength; backfill; coal pillar; unfilled zone; elastic mechanics; production safety



**Citation:** Ning, S.; Lou, J.; Wang, L.; Yu, D.; Zhu, W. Stability Influencing Factors and Control Methods of Residual Coal Pillars with Solid Waste Materials Backfilling Method. *Minerals* **2022**, *12*, 1285. <https://doi.org/10.3390/min12101285>

Academic Editor: Mamadou Fall

Received: 11 September 2022

Accepted: 12 October 2022

Published: 13 October 2022

**Publisher's Note:** MDPI stays neutral with regard to jurisdictional claims in published maps and institutional affiliations.



**Copyright:** © 2022 by the authors. Licensee MDPI, Basel, Switzerland. This article is an open access article distributed under the terms and conditions of the Creative Commons Attribution (CC BY) license (<https://creativecommons.org/licenses/by/4.0/>).

## 1. Introduction

In recent years, safety issues caused by the instability of the remaining coal pillars have increasingly received attention [1,2]. For a long time, there have been many small coal mines in western China, usually using the room-and-pillar mining method to mine coal resources [3–5]. To obtain the maximum economic profit, only better coal seams are mined. This practice has resulted in many goafs and coal pillars in the coalfield, thereby leaving severe safety hazards for large-scale coal mining today. With the integration of coal enterprises and the upgrading of mining technology, the scale of mining is steadily increased. Under the disturbance of mining activities, these pillars are prone to instability and failure, which in turn lead to mine disasters. In recent years, the instability of coal pillars caused by mining disturbance has emerged consecutively, and the treatment of the empty areas of coal pillars has become an unresolved problem [4,6].

Owing to the support of the remaining coal pillars, the roof strata form a stable state [7]. With the second mining of the coal seams in this area, the coal pillars have entered the stage of deformation and failure expansion and eventually become unstable [8,9]. The destruction of a single coal pillar will cause the destruction of the coal pillar group and eventually the continuous destruction of the coal pillars in the goaf, thereby leading to a rock burst accident [10]. The strength of the coal pillar will decline under the influence of

various factors, and this fact must be considered in the calculation [11]. The relationship between the load of the overlying strata and the stability of the remaining coal pillars must be considered, especially the change of the coal pillar stress with the advancement of the working face [12,13]. Another important factor is the sustained coal pillar strength in the goaf under the wet–dry cycle environment of the goaf [14]. When a single coal pillar is destroyed, the load borne by this coal pillar is transferred to the adjacent one, thereby resulting in the instability of the whole coal pillar group [15–17].

At the same time, many scientists have been trying to prevent and control the remaining coal pillar disasters. It has previously been observed that mining activities have an impact on the maximum vertical stress of the coal pillar, and it is possible to maintain the stability of the coal pillar by calculating the maximum stress [18]. The coal pillars first fail in a certain area, and their failure gradually spreads. By strengthening the area, the stability of the coal pillars during the mining stage can be guaranteed [19].

At the same time, research into the backfilling method has been the focus for innovation. Tesarik [20] monitored the long-term stability of coal pillars and pointed out that the backfilling method is helpful for maintaining the stability of pillars and limiting their deformation. Some experts conducted research on the physical properties of the backfilling body [21], analyzed the interaction between coal pillars and the backfilling body, and concluded that the physical and mechanical properties of the backfilling body affect the peak strength of the coal pillars as well as the post-peak intensity [22,23]. Mo [24] analyzed the influence of different filling amounts, filling types, and backfilling body sizes on goaf roof and coal pillars and proposed different filling strategies.

Through various studies, the failure characteristics of the remaining coal pillars were evident, and a relatively complete prevention method was formed. However, these studies are based on the coal pillars that are entirely exposed or the goafs that are full. No previous study has investigated the effect of an unfilled zone. When the height of the unfilled zone is large, the coal pillars may remain unstable.

Through various research studies, the damage- and disaster-causing mechanism of the remaining coal pillars have been determined, and a complete prevention method has been formed. However, these studies were based on the complete backfilling of the goaf and did not fully consider the problem of incomplete backfilling under actual conditions. When the backfill body height is small, there is a greater possibility of destabilizing the remaining coal pillars, leading to safety accidents.

The main objective of this paper is to analyze the effect of the strength and height of the backfill body on the coal pillar strength when reinforced by backfilling methods, moreover, to use this as a basis for discussing solid waste material backfilling methods.

## 2. Current Status and Treatment of Remaining Coal Pillars

### 2.1. Current Status of Coal Pillars in Goaf

The Yuanbaowan coal mine is in the Shanxi province of China. The mine was formed by the reorganization and integration of the Yuanbaowan mine and Shangmangou coal mine. Before the integration, the two mines were dominated by room-and-pillar mining methods, thereby leaving many room-and-pillar mining goafs. In the eastern part of Figure 1, the goaf of coal seam No. 9 reached 94,500 m<sup>2</sup>, and the length of the old roadway was approximately 6800 m. There were 16 goafs formed by mining, and the volume of each goaf was approximately 48,000 m<sup>3</sup>.

The 6107 working face was seriously affected by the goaf. Figure 1 shows the relative positional relationship between the working face and the goaf. The 6107 working face is in coal seam No. 6, and the average vertical distance from coal seam No. 9 is 15 m, with an inclination of 4–8°. Coal seam No. 9 has many goafs and coal pillars; the maximum width of them is 27 m and the height is between 5 m and 9 m. Some small coal pillars, with a minimum width of 6 m and an average of approximately 10 m, are left between the goafs. The length of the goaf distribution area is 240 m.

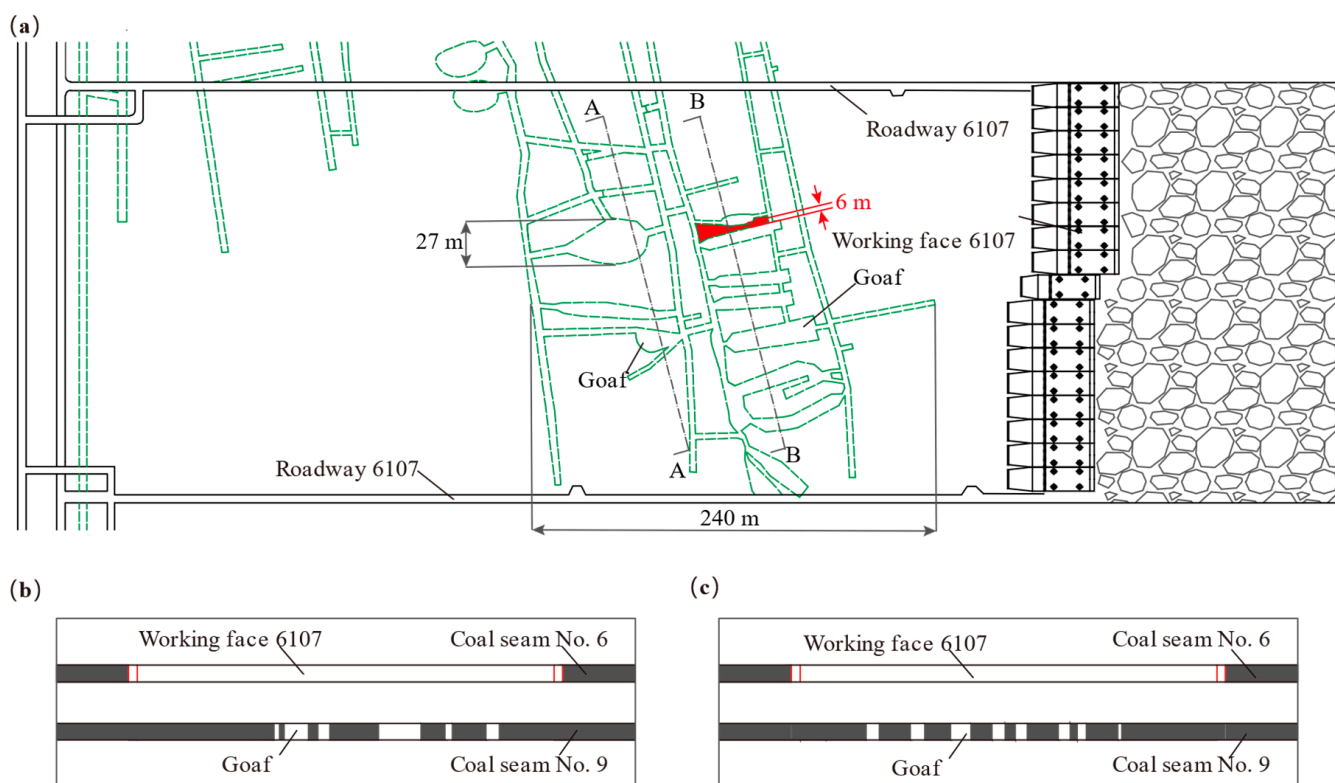


**Figure 1.** Relative positional relationship between the coal pillar and 6107 working face [25] (a) Face plan of 6107 working face (b) Sectional drawing at section line A (c) Planning view at section line B.

According to the geological data of the mine (Table 1), there is fine-grained sandstone with a thickness of 8.4 m on the top of coal seam No. 9 (depth 174.60 m), and the roof has good integrity and high strength. Early investigations revealed that the goaf is still in a good and complete state, and there is no large-scale collapse or failure. The goaf is relatively flat and has a small amount of stagnant water, which can meet the needs of personnel passage. When the 6107 working face passes over the goaf, the remaining coal pillars fail and become unstable.

**Table 1.** YZK2101 drill hole.

Lithology	Depth (m)	Thickness (m)	Rock Quality Designation
Coal seam No. 6	152.30	3.50	
Sandy mudstone	156.24	3.94	30%
Fine-grained sandstone	166.20	9.96	52%
Coal seam No. 9	174.60	8.40	
Fine-grained sandstone	175.28	0.68	
Mudstone	177.40	2.12	28%
Sandy mudstone	188.20	9.60	53%
Coal seam No. 11	189.10	0.9	

### 2.2. Governance Method

Room-and-pillar mining goaf backfilling could solve the problem of failure and instability of the remaining coal pillars [26–28]. The main process is illustrated in Figure 2. The backfilling body (fly ash and cement) is mixed in a certain proportion on the ground and injected into the goaf by means of pipeline transportation through ground drilling. Because the goaf space is interconnected, the filling material slurry flows to all parts of the goaf.

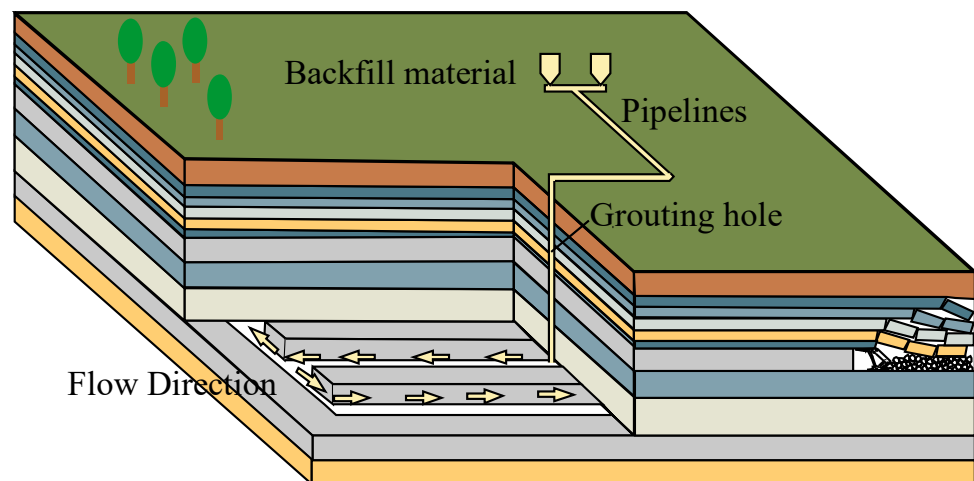


**Figure 2.** Sketch map of goaf backfilling.

The backfilling body can restrain the deformation of the surrounding rock in the goaf. Under ideal conditions, the backfilling material can fill the goaf and restrain the deformation of the surrounding rock and roof. Because it is difficult to accurately calculate the amount of backfilling material and monitor the grouting situation in real time, there is always a certain unfilled zone. In the unfilled zone, the coal pillars are still exposed, and there is a risk of failure. Therefore, it is necessary to consider controlling the height of the unfilled zone to ensure that the coal pillar has sufficient strength.

### 3. Influence Factors of Backfill Method on the Stability of Remaining Coal Pillars

#### 3.1. Numerical Simulation Test Scheme

##### 3.1.1. Numerical Model

PFC2D was used to study coal pillars' strength and failure characteristics under different conditions. The study coal pillar is in coal seam No. 9 with an overlying rock thickness of 166.20 m. The size of the numerical model was 6 m wide and 9 m high. A total of 12,506 round particles of different scales were built. The radius of the smallest particle was 0.04 mm, and the radius of the largest particle was 0.045 m.

Six walls were set up when building the numerical model (Figure 3). Walls No. 1 and No. 2 were used to simulate the sinking of the roof and floor, and the loading speed of No. 1 was 0.02 m/s. The FISH language was used to test the model strength forces and calculate the numerical magnitude of the stresses on the coal pillars based on the magnitude of the forces and the real-time width of the model. Walls No. 3 and No. 4 were used to simulate the backfilling bodies on both sides, and servo control was adopted in the subsequent calculation process. Walls No. 5 and No. 6 were in the unfilled zone and deleted after the initial balance. In the uniaxial compression test, the walls on both sides (No. 3, No. 4, No. 5, and No. 6) were deleted to simulate the failure characteristics of the coal pillar under uniaxial compression. When it was necessary to impose confining pressure on the coal pillar, walls No. 5 and No. 6 were deleted, and walls No. 3 and No. 4 were set on both sides of the coal pillar as servo walls.

##### 3.1.2. Parameter Calibration

To obtain suitable numerical model parameters, the strength of the coal sample was tested. The coal sample was derived from the Yuanbaowan coal mine. A large piece of uncracked coal was selected and transported to the laboratory to be processed into a standard specimen. Uniaxial compression tests were conducted on the MTS C64.106 rock mechanics test system (MTS Systems Corporation, Eden Prairie, MN, USA).

Table 2 shows the uniaxial compressive strength (UCS) and elastic modulus of the coal samples. The UCS ranges from 9.77 MPa to 11.44 MPa, and the elastic modulus ranges from

0.76 GPa to 0.95 GPa. The average values of the UCS and elastic modulus are 10.03 MPa and 20.81 GPa, respectively.

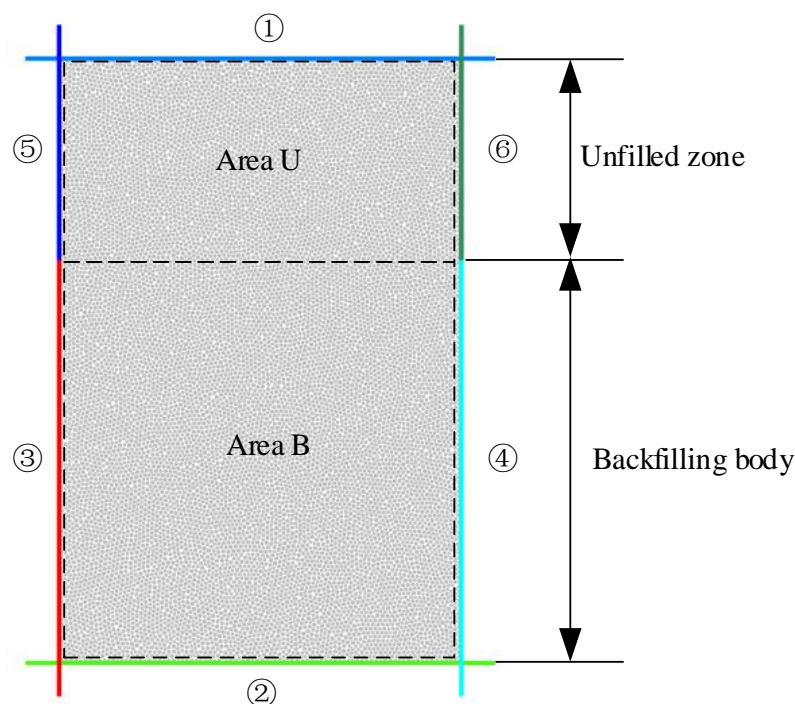


**Figure 3.** Numerical simulation model of coal pillars under different backfill body height.

**Table 2.** Strength and deformation characteristics of coal samples.

Samples	Uniaxial Compression Strength (MPa)	Elastic Modulus (GPa)	Average Strength (MPa)	Average Modulus (GPa)
C-1	7.60	0.818	9.13	0.858
C-2	11.60	1.025		
C-3	8.18	0.730		

To reflect the mechanical strength of the coal pillars in the Yuanbaowan coal mine accurately, the parameters of the mechanical model were adjusted to be close to the strength of the mechanics test (Figure 4). The contact model adopted a linear parallel bond model. The UCS of the numerical model was 9.79 MPa, and the elastic modulus was 0.82 GPa. The trial-and-error method was used to adjust the numerical simulation parameters so that the numerical simulation parameters were similar to the rock test parameters. The micromechanical parameters of the coal are listed in Table 3.

### 3.1.3. Experimental Scheme

The simulations were analyzed in terms of both backfill body height and backfill binding force. The backfill height of 1–9 m was simulated at 1 m intervals for different backfill conditions. Considering the depth of the coal seam is about 160 m when the horizontal and vertical stress is 1:1, the maximum horizontal stress of the coal seam is about 3.8 MPa (rock capacity is 2400 KN/m<sup>3</sup>). The surrounding pressure was also simulated at 1 MPa intervals for four scenarios ranging from 0 MPa (no filling) to 3 MPa. The test scheme is shown in Table 4, with a total of 28 sets of numerical simulations.

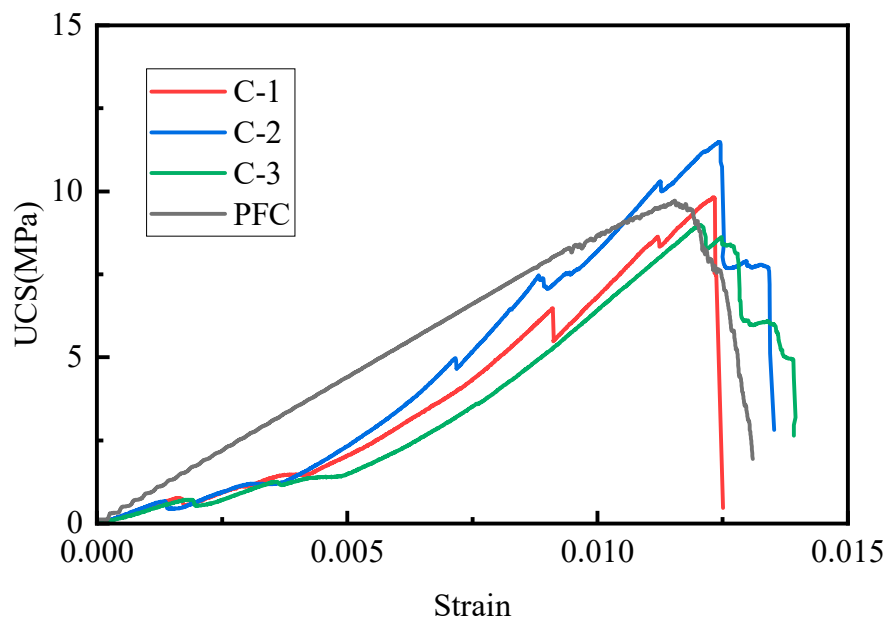


Figure 4. Coal and numerical model stress–strain curve.

Table 3. Micromechanical parameters of coal.

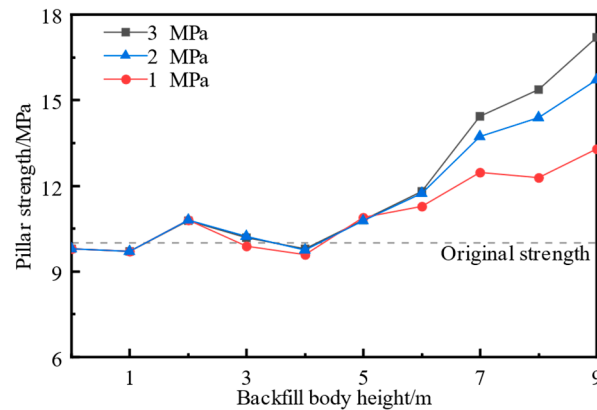
Mesomechanical Parameters	Value
Friction coefficient	0.4
Density/(kg·m <sup>-3</sup> )	2500
Friction coefficient/GPa	0.5
Normal-to-shear stiffness ratio	3
Bond effective modulus/GPa	0.5
Tensile strength/MPa	6.5
Cohesion/MPa	4
Bond normal-to-shear stiffness ratio	0.5
Normal-force update mode	1

Table 4. Numerical simulation test parameters.

No.	Confining Pressure (MPa)	Backfill Body Height (m)	No.	Confining Pressure (MPa)	Backfill Body Height (m)
1	0	0	15	2	5
2	1	1	16	2	6
3	1	2	17	2	7
4	1	3	18	2	8
5	1	4	19	2	9
6	1	5	20	3	1
7	1	6	21	3	2
8	1	7	22	3	3
9	1	8	23	3	4
10	1	9	24	3	5
11	2	1	25	3	6
12	2	2	26	3	7
13	2	3	27	3	8
14	2	4	28	3	9

### 3.2. Influence of the Unfilled Zone Height on the Strength of Coal Pillar

In order to analyze the peak coal pillar strength under different scenarios, the maximum strength of the coal pillar is monitored in each calculation. The variation pattern of peak coal pillar strength under different conditions is shown in Figure 5.



**Figure 5.** Coal pillar strength under different height conditions.

According to the results of Figure 5, as the backfill body height increases, the strength of the coal pillar increases gradually. When the backfill body height is less than 5 m, the coal column strength is close to the strength in UCS. When the backfill body height is 7 m and 8 m, the coal pillar strength increases to more than 12 MPa. When the backfill body height is 9 m, the coal column strength is the largest currently.

At the same time, the strength of the coal pillars increases as the confining pressure increases. When the backfill body height is less than 5 m, the strength of the coal pillars under different confining pressures is the same. When the backfill body height is 6 m, the strength of the coal pillars begins to differentiate. Under a confining pressure of 3 MPa, the strength of the coal pillar is 11.81 MPa. Under a confining pressure of 1 MPa, the strength of the coal pillar is 11.28 MPa. The strength appears to increase when the backfill body height is 7 m and 8 m. Under the confining pressure of 3 MPa, the strength of the coal pillar is 14.44 MPa and 15.38 MPa, respectively. Under the confining pressure of 1 MPa, the coal pillar strengths are 12.28 MPa and 12.47 MPa.

This result implies that the strength of the coal pillar is affected by both the confining pressure and backfill body height. When the backfill body height is large, the strength of the coal pillar is affected by the confining pressure. When the backfill body height is larger than 7 m, the strength of the coal pillar changes most obviously.

### 3.3. Correlation Analysis of Factors Influencing the Stability of Remaining Coal Pillars

To investigate the effect of the backfill body height and the confining pressure on coal pillar strength, we used correlation analysis to the strength and direction of the statistical correlation between backfill body height and confining pressure on coal pillar strength. The correlation of variables uses the Pearson correlation coefficient and Spearman's rank correlation coefficient. The values range from  $-1$  to  $+1$ , with  $0$  indicating no correlation between the two variables, positive values indicating a positive correlation, and negative values indicating a negative correlation, with larger values indicating a stronger correlation.

Spearman's rank correlation coefficient is suitable for the detection of variables with monotonic relationships. The Pearson correlation coefficient is suitable for the detection of normally distributed variables. The normal distribution test was performed on the backfill body height, the confining pressure, and the coal pillar strength (Table 5). According to the calculated results, the asymptotic significance was 0.200, 0.004, and 0.002, respectively. The significant coefficients of the confining pressure and coal pillar strength were less than 0.05 and did not obey the normal distribution. Therefore, we used Spearman's rank correlation coefficient.

**Table 5.** Kolmogorov–Smirnov test.

		Backfill Body Height	Confining Pressure	Coal Pillar Strength
Normal parameter	Average value	4.8214	1.9286	11.6741
	Standard deviation	2.74946	0.89974	2.13065
Most extreme difference	Absolute value	0.107	0.206	0.215
	Positive values	0.103	0.206	0.215
	Negative values	−0.107	−0.205	−0.163
Test statistics		0.107	0.206	0.215
Asymptotic significance		0.200	0.004	0.002

As shown in Table 6, the correlation coefficient between backfill body height and coal pillar strength is 0.806, which is a strong correlation. The correlation coefficient between the confining pressure and the coal pillar strength is 0.161, which is a poor correlation. This result indicates that the backfill body height has the most significant influence on the stability of the coal pillar. Controlling the backfill body height could improve the strength of the coal pillar and reduce the risk of coal pillar instability.

**Table 6.** Spearman’s rank correlation coefficient.

		Backfill Body Height	Confining Pressure	Coal Pillar Strength
Backfill body height	Correlation coefficient	1.000	-	0.861
	Sig.	-	-	0.000
	N	28	-	28
Confining pressure	Correlation coefficient	-	1.000	0.161
	Sig.	-	-	0.414
	N	-	28	28

**4. Solid Waste Material Backfill Method**

*4.1. Mechanical Model Construction and Calculation*

4.1.1. Mechanical Model Construction and Calculation

The coal pillars mainly bear the overburden load and the restraint stress of the backfill body. As shown in Figure 6, any concentrated force  $P$  acting on the boundaries on both sides of the coal pillar generates additional stress inside the coal pillar. As the distance from the surface of the coal pillar increases, the range of the additional stress distribution gradually increases. Therefore, although there are blank spaces on both sides of the pillars, they are still affected by the restraint stress.

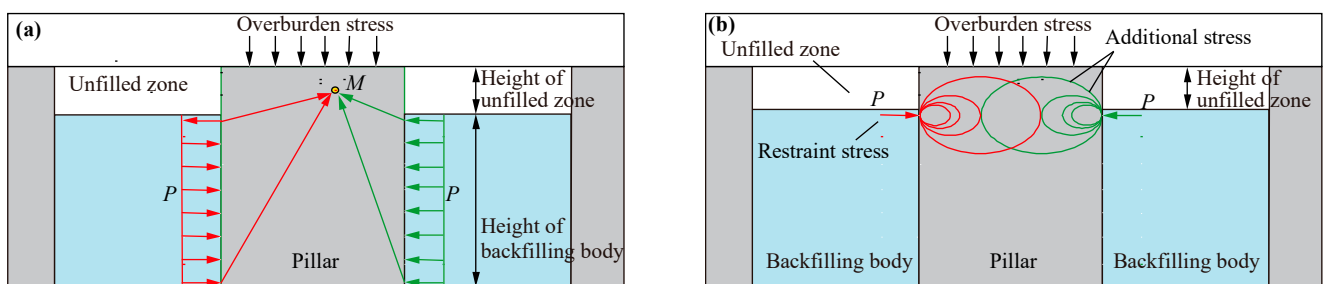


**Figure 6.** Mechanical model of lateral restraint of filling material. (a) Coal pillar force model, (b) half-plane model.

If the additional stress on the top of the coal pillar is large, the transverse deformation is suppressed. The strength of the coal pillars can be significantly increased, which can support the roof more effectively. If the additional stress in this area is small, the coal pillars are further damaged under a heavy load, which eventually leads to instability.

For any point M in the coal pillar (Figure 6a), the additional stress acting on this point derives from the restraint stress on both sides of the coal pillar. Because the additional stresses on both sides of the coal pillar are independent and symmetrical, the restraint stress on the one side of the coal pillar is studied to simplify the study.

To analyze the transfer law of the horizontal restraint stress, the coal pillar is regarded as a half-plane body. Suppose the horizontal restraint stress of the backfilling body on the coal pillar is  $P$  and acts on the boundary evenly. A schematic diagram of the built mechanical model is illustrated in Figure 6b.

Regarding the top interface of the backfilling body as the dividing line, there is a uniformly distributed stress on the lower boundary of the coal pillar. The intersection of the top boundary of the backfilling body and the coal wall is the coordinate origin O, the positive semi-axis of  $y$  is the unfilled zone, and the negative semi-axis is the backfilling body. At the same time, let the height of the unfilled zone be  $h_u$  and the height of the backfilling body be  $h_b$ .

On the  $y$ -axis, at the distance  $\zeta$  from point O, consider a tiny length  $d\zeta$ . Regarding the stress  $dp = qd\zeta$  on it as a tiny concentrated force, the stress caused by each concentrated force at a point M ( $x, y$ ) in the plane is

$$d\sigma_x = -\frac{2Pd\zeta}{\pi} \frac{x^3}{[x^2 + (y - \zeta)^2]^2} \quad (1)$$

where  $\sigma_x$  is the horizontal additional stress at this point (MPa).

If the integration interval is  $[-h_b, 0]$ , the stress concentration at each point is  $P$ , thus the horizontal additional stress at any point in the coal pillar is

$$\sigma_x = -\frac{2}{\pi} \int_{-h_b}^0 \frac{Px^3 d\zeta}{[x^2 + (y - \zeta)^2]^2} \quad (2)$$

From this, the horizontal additional stress expression at any point M in the coal pillar can be obtained as

$$\sigma_x = -\frac{P}{\pi} \left[ \arctan \frac{y + h_b}{x} - \arctan \frac{y}{x} + \frac{x(y + h_b)}{x^2 + (y + h_b)^2} - \frac{xy}{x^2 + y^2} \right] \quad (3)$$

Hence, the stress concentration factor at each point is

$$\lambda = \frac{\sigma_x}{P} \quad (4)$$

where  $\sigma_x$  is the stress concentration factor at this point.

#### 4.1.2. Mechanism of the Influence of Backfilling Body on the Coal Pillars in the Unroofed Area

The coal pillars mainly bear the pressure from the overlying strata and generate additional stress in the coal pillar. According to the Mohr–Coulomb criterion, the ultimate compressive strength of the coal pillar under one-point compression can be obtained as

$$\sigma_1 = \frac{2c \cos \varphi}{1 - \sin \varphi} + \sigma_3 \frac{1 + \sin \varphi}{1 - \sin \varphi}$$

where  $\varphi$  is the internal friction angle of coal ( $^\circ$ ),  $c$  is the cohesive force of coal (MPa),  $\sigma_3$  is the additional stress at this point (MPa), and  $\sigma_1$  is the ultimate compressive strength at this point (MPa).

After filling, a horizontal restraint stress is generated and acts on the coal pillar. Consequently, additional stress is generated inside the coal pillar. Substituting the additional stress into the above equation, the strength of this point can be calculated as

$$\sigma_1^* = \frac{2c \cos \varphi}{1 - \sin \varphi} + (\sigma_3 + \lambda P) \frac{1 + \sin \varphi}{1 - \sin \varphi}$$

Among them, the increment produced by the additional stress  $\Delta\sigma_1^*$  is

$$\Delta\sigma_1^* = \lambda P \frac{1 + \sin \varphi}{1 - \sin \varphi}$$

It is apparent that the strength of each point in the coal pillar increases with the additional stress  $\sigma_x$ . When the height of the backfilling body is determined, the stress concentration factor at any point is determined as well. Therefore, increasing the horizontal restraint stress could increase the additional stress inside the coal pillar, thereby increasing the strength at the point.

For the coal mass in the unfilled zone, the additional stress generated by the restraint stress is different, thereby resulting in a large difference in the strength at each point. To illustrate this problem, consider the example of the three points A, B, and C shown in Figure 7.

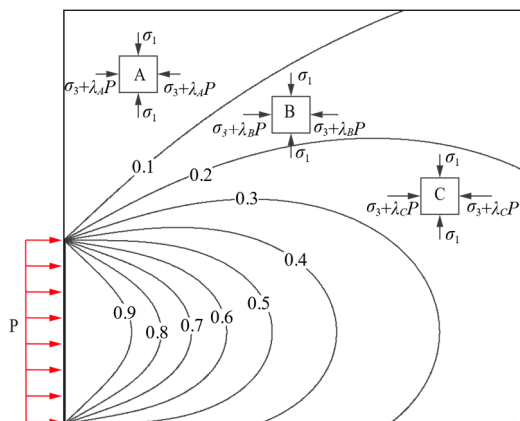


Figure 7. Influence of additional stress at each point in the coal pillar.

Among these points, the additional stress concentration factor  $\lambda_A$  at point A is smallest, the additional stress concentration factor  $\lambda_B$  at point B is larger, and the additional stress concentration factor  $\lambda_C$  at point C is largest. When the coal mass is located at point A, it is least affected by the additional stress, the ultimate strength increase is smallest, and the failure is most likely to occur. When the coal mass is at point B, it is most affected by the additional stress value, and the ultimate strength increase increases, thereby making it harder to fail. When the coal mass is at point C, it is most affected by the additional stress value, the ultimate strength increase is largest, and the strength is highest.

Because the edges of coal pillars are most prone to failure, to maintain the stability of the coal pillars, the stability of the elastic core zone must be ensured. Under the heavy load, the coal pillar has a plastic failure zone and an elastic core zone from the coal wall to the deep part. To keep the coal pillars stable, the elastic core zone should be within the influence range of the additional stress to ensure that the elastic core zone obtains a larger horizontal restraint stress, and thus the coal pillar has a higher bearing capacity.

#### 4.2. Height of Solid Waste Material Backfill Body

##### 4.2.1. Influence of the Backfill Body Height on the Distribution of Additional Stress in Coal Pillar

To further analyze the influence of the backfill body height on the additional stress distribution, calculations were performed for the backfill body heights of 5 m, 6 m, 7 m, and 8 m. The calculation results are depicted in Figure 8.

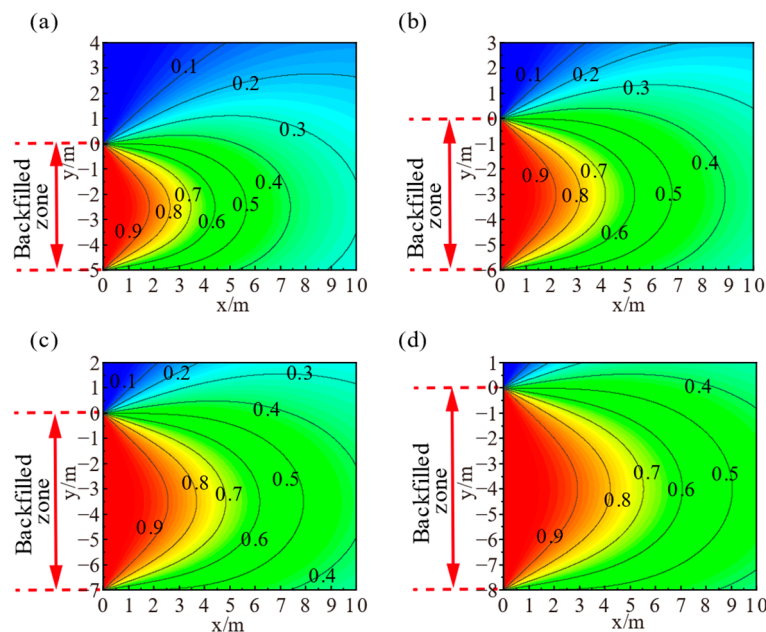


**Figure 8.** Contours of additional stress distribution in coal with different backfill body heights. (a) 5 m, (b) 6 m, (c) 7 m, (d) 8 m.

As it can be noticed in Figure 8, as the backfill body height increase, the low-stress zone of the coal pillar decreases significantly, and the additional stress at each point increases significantly. When the backfill body height is 5 m, the areas with concentration factors less than 0.1 and 0.2 account for 10.32% and 22.95% of the total area, respectively. When the backfill body height is 6 m, the areas with concentration factors less than 0.1 and 0.2 are reduced to 5.68% and 10.27% of the total area, respectively. When the backfill body height is 7 m, the areas with concentration factors less than 0.1 and 0.2 account for 2.62% and 4.33% of the total area, respectively. When the backfill body height is 8 m, these two values fall to 0.84% and 1.26%, respectively.

As the backfill body height increases, the stress value at the top boundary continues to increase. When backfill body height is 5 m, the additional stress concentration factor of the top boundary is less than 0.2 and its average value is 0.09. When backfill body height is 6 m and 7 m, the additional stress concentration factor of the top boundary is between 0.2 and 0.3 and the average values are 0.13 and 0.19, respectively. When backfill body height is 8 m, the additional stress concentration factor in the larger area of the top boundary is more than 0.3 and the average value is 0.28. Compared to other areas inside the coal pillar, the additional stress at the top boundary is still relatively small.

##### 4.2.2. Distribution Law of Additional Stress at the Top Boundary

Because the top boundary of the coal pillar is a weak area of the coal pillar, the change law of the additional stress must be studied. Figure 9 shows the change law of additional stress at the top boundary under different conditions.

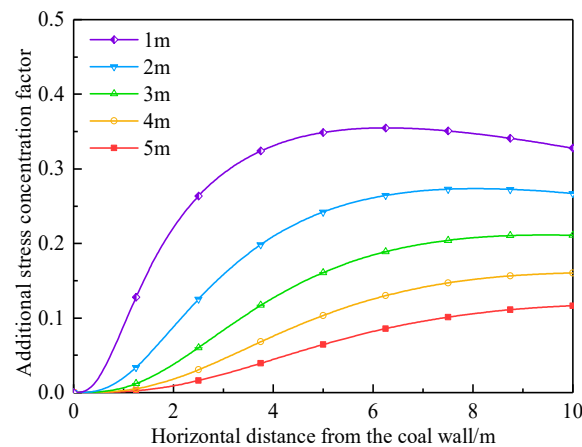


**Figure 9.** Variation law of additional stress concentration factor at the top interface of coal pillar under different conditions.

As shown in Figure 9, as the horizontal distance from the coal wall increases, the stress concentration factor gradually increases from zero. When the horizontal distance reaches 8 m, the curves enter a stable stage. As the backfill body height increases, the growth rate of each curve increases. When the backfill body height is less than 7 m, the stress concentration factor increases slowly. The growth rate of the stress concentration factor is most obvious when the backfill body height is more than 7 m.

In the stable stage, as backfill body height decreases, the additional stress concentration factor gradually decreases. When the height of the unfilled zone is 8 m, the maximum concentration factor is 0.35. When the height is 7 m, 6 m, and 5 m, the stress concentration factor is 0.27, 0.21, and 0.16, respectively, which means a reduction of 22.98%, 40.5%, and 54.8%, respectively.

#### 4.2.3. Variation of Additional Stress in the Elastic Core Area of Coal Pillar

Considering the minimum width of the coal pillar in the Yuanbaowan coal mine as an example, the distance between the central axis and the coal wall is 3 m. According to the previous calculation results, the stress concentration factor at the center of the coal pillar reaches its minimum at the top interface, thus the most dangerous situation is used for calculation. The results are presented in Figure 10.

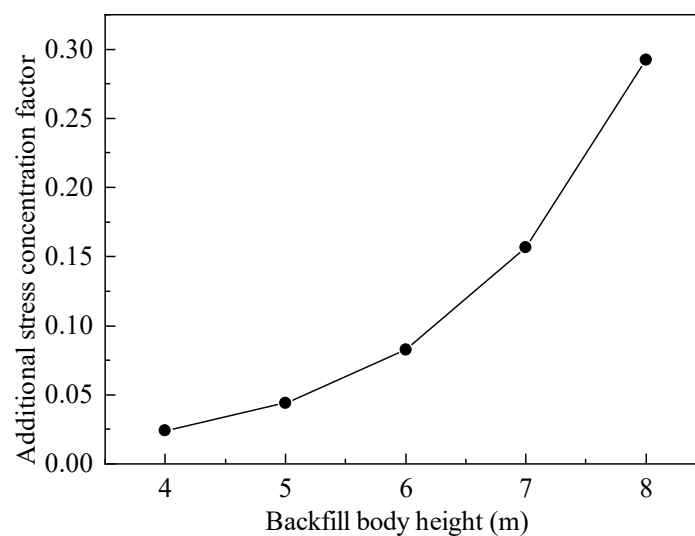


**Figure 10.** Additional stress on the central axis of coal pillars with different backfill body heights.

In the elastic core zone, the stress concentration factor increased with the backfill body height. Regarding the backfill body height of 8 m as the benchmark, when the height decreases to 7 m, the additional stress decreases by 46.1%. As the height decreases to 6 m, the additional stress decreases by 71.6%. When the height decreases to 5 m and 4 m, the additional stress is reduced by 84.7% and 91.6%, respectively. This result implies that when the backfill body height is larger than 7 m, the additional stress in the elastic core zone increases significantly.

In summary, to ensure the strength of the elastic core zone, the additional stress in the elastic core zone of the coal pillar should be made more significant. Moreover, it can be ensured that the elastic core zone is entirely within its stress influence range. When the height of the filled zone is less than 2 m, the exposed area is more affected by the additional stress and is able to maintain better integrity. Therefore, when filling, it is essential to ensure that the height of the unfilled zone is less than 2 m.

#### 4.3. Solid Waste Backfill Material Proportioning Analysis

To obtain the mechanical characteristics of the coal and the backfill material, standard specimens of backfill material were prepared for uniaxial compression tests.

##### 4.3.1. Sample Preparation

The backfill body specimen was made of fly ash and cement. According to the different typical proportions of cement and fly ash (1:2, 1:3, 1:4, 1:5, 1:6), a total of five different samples were prepared. First, the cement and fly ash were weighed according to the proportion, mixed, and stirred evenly. Subsequently, the mix was introduced into the specimen mould to make a standard specimen. The specimens were cured for 28 days after production. The cement is common Portland cement (GB 175-2007 (GB175-2007)) with a compressive strength of 42.5 MPa.

##### 4.3.2. Experimental Equipment and Procedure

Uniaxial compression tests were conducted on the MTS C64.106 rock mechanics test system (MTS Systems Corporation, Eden Prairie, MN, USA), as shown in Figure 11. The test adopted displacement control, and the loading speed was 0.3 mm/min.



**Figure 11.** Loading system. (a) Experimental system, (b) uniaxial compression.

##### 4.3.3. Mechanical Test Results

Table 7 shows the uniaxial compressive strength and deformation characteristics of the backfilling body. There is a negative correlation between the backfilling body uniaxial compressive strength and the proportion of fly ash. As the proportion of fly ash increases, the uniaxial compressive strength gradually declines. When the ratio of cement to filler is 1:2 and 1:6, the strength reaches the maximum and minimum value, respectively. The maximum and minimum filling strengths are 0.661 MPa and 3.862 MPa, respectively.

**Table 7.** Strength and deformation characteristics of backfilling body samples with different Cement/fly ash ratios.

Group	Samples	Cement/Fly Ash Ratios	Uniaxial Compression Strength (MPa)	Elastic Modulus (GPa)	Average Strength (MPa)	Average Modulus (GPa)
1	f-11	1:2	3.719	0.015468	3.862	0.014997
	f-12		3.750	0.020028		
	f-13		4.117	0.009494		
2	f-21	1:3	1.921	0.013762	2.039	0.011939
	f-22		2.211	0.011058		
	f-23		1.987	0.010998		
3	f-31	1:4	1.385	0.010716	1.439	0.009105
	f-32		1.233	0.007286		
	f-33		1.701	0.009314		
4	f-41	1:5	0.922	0.007294	0.696	0.010309
	f-42		0.417	0.008936		
	f-43		0.749	0.014698		
5	f-51	1:6	0.478	0.002718	0.661	0.005809
	f-52		0.570	0.008492		
	f-53		0.937	0.006216		

#### 4.4. Proportioning of Solid Waste Backfill Materials

In order to ensure the safety of the overburden working face, the strength of the remaining coal pillar needs calibrated first. According to the article [29], the vertical stress concentration coefficient of the floor varies greatly at different depths during the mining process. At a depth of 15 m in the floor, the maximum stress concentration factor is 1.44. Calculated in accordance with the mining retention ratio of 1:1, a single coal pillar will bear half of the weight of each side goaf. The maximum stress concentration factor during mining is 2.88. This is greater than the uniaxial compressive strength of the coal pillar of 10.03 MPa.

In order to avoid destabilization of the coal pillar, it should be ensured that the elastic core of the pillar remains strong under peak stress. Therefore, the backfill materials in the goaf should not be damaged during large deformations of the coal column. This requires the backfill material peak stress greater than the confining pressure required to maintain the strength of the coal pillar.

Based on the analysis in Section 3.1, the peak strength of the backfill material is brought into Equation (2). The strength of the coal pillar after backfilling was calculated based on the results of the mechanical tests in Section 2.1. The internal friction of the coal is taken as 40°. Based on this method, the maximum strength of the coal pillar after backfilling can be calculated and the results of the calculation are shown in Table 8.

**Table 8.** Coal pillar strength for different filling material proportioning scheme.

No.	Cement/Fly Ash Ratios	Pillar Strength (MPa)
1	1:2	13.34
2	1:3	12.00
3	1:4	11.56
4	1:5	11.02
5	1:6	11.00

According to Equation (1), the coal pillar peak strength is 11.57 MPa when using a ratio of 1:4. This value is greater than the maximum ground stress of 10.51 MPa and is approximately 105.60% of the stress. Considering the surplus factor, cement/fly = 1:4 was chosen to ensure a good strength of the coal pillar.

## 5. Field Application Results

After backfilling, the borehole TV was suspended along the grouting borehole into the extraction zone to observe the backfilling condition (Figure 12). The depth below the drill TV is recorded using the grout hole opening as the starting point for observation (0 m). When the borehole TV is lowered to the bottom of the hole, record the depth of the borehole TV. The depth at the bottom of the hole is used as the elevation of the top interface of the goaf. As there is a small amount of water in the goaf, the water surface is used as the top interface of the backfilling. When there is an unfilled zone, the backfill body height can be calculated from these data.



Figure 12. Live peep operations [30–32]. (a) Daily observations, (b) Goaf peep results.

When the goaf is filled with backfill material, the borehole television cannot be lowered. Therefore, when the water surface was observed, the goaf was considered to be filled. Due to some of the boreholes being misaligned or collapsed, only four boreholes were probed (No. 1, No. 5, No. 6, and No. 13), and Table 9 shows peephole results.

Table 9. Observations from different boreholes [30,31].

No.	Depth to Bottom of Hole (m)	Water Depth (m)	Backfill Body Height (m)	Unfilled Zone Height (m)	If Instability Occur
1		−65	9	0	No
5	−160.5	−162.7	6.8	2.2	No
6		−159	0	0	No
13	−164.2	−167.8	5.4	3.6	Yes

Based on this result, coal mining can be carried out generally in two cases, when the goaf is filled, or the unfilled zone height is less than 2 m. The floor collapses when the unfilled zone height is larger (No. 13), which seriously affects the safety of coal mining activities.

## 6. Conclusions

- (1) The solid waste material backfill will maintain the stability of the remaining coal pillars in the bottom bunker. The height of the backfill body is the main factor affecting the stability of the coal pillar. When the backfill body height is large, the strength of the coal pillar is close to the strength when it is filled. Too small a backfill height will not maintain the stability of the coal column. In addition, the restraint stresses acting on the coal pillar can effectively control the deformation and damage of the pillar. The strength of the coal pillar is further enhanced when higher strength filling materials are used to provide high restraint stresses.
- (2) A new backfill method for solid waste material is proposed. A half-plane model analyzes the relationship between the backfill body and the coal pillar. Calculation

of the influence of the confining stress of the filling body on the coal pillar and the reasonable backfilling height is then determined. Analyzing the strength of the coal pillar in conjunction with the Mohr–Coulomb criterion, a suitable material ratio is selected. The field tests proved that the coal pillar did not become unstable at a minimum filling height of 7 m and a cement/fly ash ratio of 1:4, which ensured production safety.

- (3) The main influencing factors of solid waste material backfill reinforcement of remaining coal pillars were determined. We used Spearman’s rank correlation coefficient to calculate the correlation between the backfill body height and coal pillar strength and the correlation between the confining pressure and coal pillar strength. The results show that the backfill body height is the most critical factor affecting the coal pillar strength. The backfill body strongly correlates with the coal pillar strength (correlation coefficient of 0.806).

**Author Contributions:** Conceptualization, W.Z. and S.N.; methodology, S.N., L.W. and J.L.; software, S.N. and L.W.; validation, D.Y. and L.W.; formal analysis, S.N. and J.L.; investigation, L.W.; resources, W.Z.; data curation, L.W. and J.L.; writing—original draft preparation, S.N.; writing—review and editing, S.N. and J.L.; visualization, W.Z.; supervision, W.Z.; project administration, W.Z.; funding acquisition, L.W. All authors have read and agreed to the published version of the manuscript.

**Funding:** This research was funded by the Open Research Fund of The State Key Laboratory of Coal Resources and Safe Mining, CUMT (SKLCRSM-XJIEKF006).

**Data Availability Statement:** Not applicable.

**Acknowledgments:** The authors would like to thank the reviewers for their constructive comments, which improved the paper, and anonymous colleagues for their kind efforts and valuable comments, which have improved this work.

**Conflicts of Interest:** The authors declare no conflict of interest.

## References

- Gao, H.; An, B.; Han, Z.; Guo, Y.; Ruan, Z.; Li, W.; Zayzay, S. The Sustainable Development of Aged Coal Mine Achieved by Recovering Pillar-Blocked Coal Resources. *Energies* **2020**, *13*, 3912. [\[CrossRef\]](#)
- Waclawik, P.; Kukutsch, R.; Konicek, P.; Kajzar, V. Monitoring of coal pillars yielding during room and pillar extraction at the great depth. In Proceedings of the International European Rock Mechanics Symposium (EUROCK), Saint Petersburg, Russia, 22–26 May 2018; pp. 711–716.
- Liu, H.F.; Sun, Q.; Zhou, N.; Wu, Z.Y. Risk Assessment and Control Strategy of Residual Coal Pillar in Room Mining: Case Study in Ecologically Fragile Mining Areas, China. *Sustainability* **2021**, *13*, 2712. [\[CrossRef\]](#)
- Shang, T.L.; Liu, Y.W.; Suo, Y.L.; Wang, J.D.; Wang, Z.Y. Numerical Simulation on Instability Mechanism of Section Coal Pillar in Shallow Buried Coal Seams. *Teh. Vjesn.* **2022**, *29*, 108–113. [\[CrossRef\]](#)
- Shang, H.F.; Ning, J.G.; Hu, S.C.; Yang, S.; Qiu, P.Q. Field and numerical investigations of gateroad system failure under an irregular residual coal pillar in close-distance coal seams. *Energy Sci. Eng.* **2019**, *7*, 2720–2740. [\[CrossRef\]](#)
- Geng, Y.Q.; Suo, Y.L. Rational Width of Chain Coal-pillar in Shallow Coal Seam in the Northern Shaanxi Area. *Electron. J. Geotech. Eng.* **2019**, *24*, 405–412.
- Zingano, A.; Weiss, A. Subsidence over room and pillar retreat mining in a low coal seam. *Int. J. Min. Sci. Technol.* **2019**, *29*, 51–57. [\[CrossRef\]](#)
- Zhu, W.; Chen, L.; Zhou, Z.; Shen, B.; Xu, Y. Failure Propagation of Pillars and Roof in a Room and Pillar Mine Induced by Longwall Mining in the Lower Seam. *Rock Mech. Rock Eng.* **2018**, *52*, 1193–1209. [\[CrossRef\]](#)
- Zhu, W.; Xu, J.; Li, Y. Mechanism of the dynamic pressure caused by the instability of upper chamber coal pillars in Shendong coalfield, China. *Geosci. J.* **2017**, *21*, 729–741. [\[CrossRef\]](#)
- Zipf, R.K., Jr.; Mark, C. Design methods to control violent pillar failures in room-and-pillar mines. *Trans. Inst. Min. Metall. Sect. A-Min. Ind.* **1997**, *106*, A124.
- Poulsen, B.A.; Shen, B.; Williams, D.J.; Huddleston-Holmes, C.; Erarslan, N.; Qin, J. Strength reduction on saturation of coal and coal measures rocks with implications for coal pillar strength. *Int. J. Rock Mech. Min. Sci.* **2014**, *71*, 41–52. [\[CrossRef\]](#)
- Ma, Q.; Tan, Y.L.; Liu, X.S.; Gu, Q.H.; Li, X.B. Effect of coal thicknesses on energy evolution characteristics of roof rock-coal-floor rock sandwich composite structure and its damage constitutive model. *Compos. Part B-Eng.* **2020**, *198*, 108086. [\[CrossRef\]](#)
- Malli, T.; Yetkin, M.E.; Özfırat, M.K.; Kahraman, B. Numerical analysis of underground space and pillar design in metalliferous mine. *J. Afr. Earth Sci.* **2017**, *134*, 365–372. [\[CrossRef\]](#)

14. Chen, S.; Jiang, T.; Wang, H.; Feng, F.; Yin, D.; Li, X. Influence of cyclic wetting-drying on the mechanical strength characteristics of coal samples: A laboratory-scale study. *Energy Sci. Eng.* **2019**, *7*, 3020–3037. [[CrossRef](#)]
15. Zhou, Z.; Chen, L.; Zhao, Y.; Zhao, T.; Cai, X.; Du, X. Experimental and Numerical Investigation on the Bearing and Failure Mechanism of Multiple Pillars Under Overburden. *Rock Mech. Rock Eng.* **2016**, *50*, 995–1010. [[CrossRef](#)]
16. Zhou, Z.; Zhao, Y.; Cao, W.; Chen, L.; Zhou, J. Dynamic Response of Pillar Workings Induced by Sudden Pillar Recovery. *Rock Mech. Rock Eng.* **2018**, *51*, 3075–3090. [[CrossRef](#)]
17. Zhou, Z.; Chen, L.; Cai, X.; Shen, B.; Zhou, J.; Du, K. Experimental Investigation of the Progressive Failure of Multiple Pillar–Roof System. *Rock Mech. Rock Eng.* **2018**, *51*, 1629–1636. [[CrossRef](#)]
18. Yu, Y.; Deng, K.-Z.; Chen, S.-E. Mine Size Effects on Coal Pillar Stress and Their Application for Partial Extraction. *Sustainability* **2018**, *10*, 792. [[CrossRef](#)]
19. Bai, J.; Feng, G.; Wang, S.; Qi, T.; Yang, J.; Guo, J.; Li, Z.; Du, X.; Wang, Z.; Du, Y.; et al. Vertical stress and stability of interburden over an abandoned pillar working before upward mining: A case study. *R. Soc. Open Sci.* **2018**, *5*, 180346. [[CrossRef](#)]
20. Tesarik, D.R.; Seymour, J.B.; Yanske, T.R. Long-term stability of a backfilled room-and-pillar test section at the Buick Mine, Missouri, USA. *Int. J. Rock Mech. Min. Sci.* **2009**, *46*, 1182–1196. [[CrossRef](#)]
21. Zhang, K.; Li, N. A new method to replicate high-porosity weak rocks subjected to cyclic freezing-thawing: Sand 3D printing and digital image correlation explorations. *Int. J. Rock Mech. Min. Sci.* **2022**, *157*, 105174. [[CrossRef](#)]
22. Wang, H.; Poulsen, B.A.; Shen, B.; Xue, S.; Jiang, Y. The influence of roadway backfill on the coal pillar strength by numerical investigation. *Int. J. Rock Mech. Min. Sci.* **2011**, *48*, 443–450. [[CrossRef](#)]
23. Wang, X.Q.; Meng, X.R.; Gao, Z.N. Study on Reasonable Filling Width of Gob-Side Entry Retaining and its Engineering Application. *Adv. Mater. Res.* **2013**, *807–809*, 2288–2293. [[CrossRef](#)]
24. Mo, S.; Canbulat, I.; Zhang, C.; Oh, J.; Shen, B.; Hagan, P. Numerical investigation into the effect of backfilling on coal pillar strength in highwall mining. *Int. J. Min. Sci. Technol.* **2018**, *28*, 281–286. [[CrossRef](#)]
25. Yi, X.Y.; Zhu, W.B.; Ning, S.; Wang, L.L.; Luo, Z.Q. Critical Height of Unfilled Zone in Underlying Gob Piles. *Shock. Vib.* **2021**, *2021*, 6634295. [[CrossRef](#)]
26. Ning, S.; Zhu, W.; Yi, X.; Wang, L. Evolution Law of Floor Fracture Zone above a Confined Aquifer Using Backfill Replacement Mining Technology. *Geofluids* **2021**, *2021*, 8842021. [[CrossRef](#)]
27. Yu, S.; Xu, J.; Zhu, W.; Wang, S.; Liu, W. Development of a combined mining technique to protect the underground workspace above confined aquifer from water inrush disaster. *Bull. Eng. Geol. Environ.* **2020**, *79*, 3649–3666. [[CrossRef](#)]
28. Zhu, W.; Xu, J.; Xu, J.; Chen, D.; Shi, J. Pier-column backfill mining technology for controlling surface subsidence. *Int. J. Rock Mech. Min. Sci.* **2017**, *96*, 58–65. [[CrossRef](#)]
29. Ning, S. Research on Surrounding Rock Deformation and Sectional Control Technology of Roadway Crossing through Passage. Master's Thesis, Shandong University of Science and Technology, Qingdao, China, 2019.
30. Feng, G.; Zhu, W.; Li, Z.; Bai, J. Dynamic collapse mechanism and prevention of shallow buried pillar group underlying floor in kick-off mining. *Meitan Xuebao J. China Coal Soc.* **2022**, *47*, 200–209. [[CrossRef](#)]
31. Luo, Z. Study on Instability Mechanism of Floor Coal and Rock Pillars in Upward Mining above Goaf in Yuanbaowan Coal Mine. Master's Thesis, China University of Mining and Technology, Xuzhou, China, 2020.
32. Yu, D.; Yi, X.; Liang, Z.; Lou, J.; Zhu, W. Research on Strong Ground Pressure of Multiple-Seam Caused by Remnant Room Pillars Undermining in Shallow Seams. *Energies* **2021**, *14*, 5221. [[CrossRef](#)]